Structural Engineering and Mechanics, Vol. 19, No. 1 (2005) 1-20
DOI: http://dx.doi.org/10.12989/sem.2005.19.1.001

Limit load equations for partially restrained RC slabs

O. O. Olufemi† and K. L. Cheung‡

School of Engineering and Physical Sciences, University of Aberdeen, AB24 3UE, U.K.

K. M. A. Hossain‡†

Department of Civil Engineering, Ryerson University, Toronto, Ontario, Canada M5B 2K3

(Received May 27, 2002, Accepted August 20, 2004)

Abstract. The expertise required in the judicious use of nonlinear finite element (FE) packages for design-assistance purposes is not widely available to the average engineer, whose sole aim may be to obtain an estimate for a single design parameter, such as the limit load capacity of a structure. Such a parameter may be required for the design of a proposed reinforced concrete (RC) floor slab or bridge deck with a given set of geometrical and material details. This paper outlines a procedure for developing design-assistance equations for carrying out such predictions for partially restrained RC slabs under uniformly distributed loading condition, based on a database of FE results previously generated from a large number of 'numerical model' slabs. The developed equations have been used for predicting the peak loads of a number of experimental RC slabs having varying degrees of edge restraints; with results showing a reasonable degree of accuracy and low level of scatter. The simplicity of the equations makes them attractive and their successful use in the field of application reported in this paper suggest that the outlined procedure may also be extended to other classes of concrete structures.

Key words: finite elements; partially restrained RC slabs; FE-based equations; limit load prediction; numerical modeling; design assistance tools; FE predictions.

1. Introduction

Membrane action has been noted to be very significant in RC slabs especially where the edges are restrained against movement and the traditional use of the yield line method of analysis has proved inadequate to analyse such problems. For the design-assistance of frequently occurring nonlinear RC slabs, recent research effort has focused on the development of FE-based prediction tools. These tools were developed from a database of peak-load values resulting from the FE analyses of many 'numerical model' RC slabs of various boundary conditions. The tools include prediction charts and computer-assisted prediction software, for simply supported slabs (Hossain and Famiyesin 1997, 2001) and for fully and partially restrained RC slabs (Famiyesin and Hossain 1998a,b). The charts and software developed leave gaps in the parametric field, which are bridged by series of

† Lecturer
‡ Research Student
‡† Adjunct Professor

interpolation of results, thereby compromising the integrity of the solution. There is therefore the need to develop prediction equations based on the database of results from previous FE analyses carried out by the authors, involving a range of material and geometric combinations. This objective forms the focus of this paper. The quality of the developed equations is demonstrated by the strength prediction of a number partially restrained RC slabs, which have been tested by different authors.

Two methods are used in this paper to develop three prediction equations for the class of partially restrained RC slabs. The first method uses non-dimensional material and geometric parameters to generate a series of sub-system equations, from which the final prediction equation is formed. Two equations are developed by this method; the first using line of best fit and the second employing lower-bound relationships to arrive at the final equation, a process that has a built-in design consideration. The second method uses the MATLAB software, (see Herniter 2001) to form the general equation, which is directly dependent on all the relevant slab parameters. The constants associated with these parameters are identified from the database of FE results. The usefulness of the equations developed is demonstrated by their use in estimating the limit loads of a number of experimental slabs, tested by previous authors. Results from the methods outlined in this paper for partially restrained RC slabs suggest that the method could have wider applications for other engineering problems.

The term ‘partially restrained slabs’ have been used in this paper in its broad sense to include all cases where all the slab edges are supported but are neither wholly fully restrained (fixed) nor wholly simply supported (or hinged). Full restraint, as interpreted in FE analysis, is when all the degrees of freedom at the boundary nodes (including displacements and rotations) are totally prevented. In practice however different laboratories attempt to achieve the ‘fully restrained’ situation by different methods. The methods adopted may vary from the case where the slab edges are rigidly built into end supports as shown in Fig. 1(a), to the case where top ends of the slab edges are bolted to the support base while there is no lateral restraint, (see Fig. 1d). Thus for a significant number of the so-called experimental ‘fully restrained’ slabs, only about 50-90% fixity is actually achieved at the edges, (when compared with the 100% fixity assumed in FE analysis). Figs. 1 (a-d) show the laboratory representation of ‘full restraint’ at the slab edges and ‘uniformly distributed loading’, as implemented by different authors, (e.g., Wood 1961, Keenan 1969, Park 1964, Hung and Nawy 1971).

Wholly supported RC slabs which qualify as ‘partially restrained slabs’, are those specified as classes II and III in Hossain and Famiyesin (2001). The class II slab category is where three of the slab edges are ‘fully restrained’ and one edge is hinged (or simply supported, see Fig. 2a). Class III slab category on the other hand is where one pair of adjacent edges are ‘fully restrained’ and the other pair are hinged (or simply supported, see Fig. 2b). Examples of the classes II and III slabs considered in this paper are those tested by Park (1964), Hung and Nawy (1971) and Nawy and Blair (1971).

2. Finite element modeling

The full details of the FE modelling for partially restrained slab have been reported in Famiyesin and Hossain (1998b). The model is based on a 3D degenerated, layered shell element formulation with each element having 8 or 9 nodes, and each node having five degrees of freedom; three

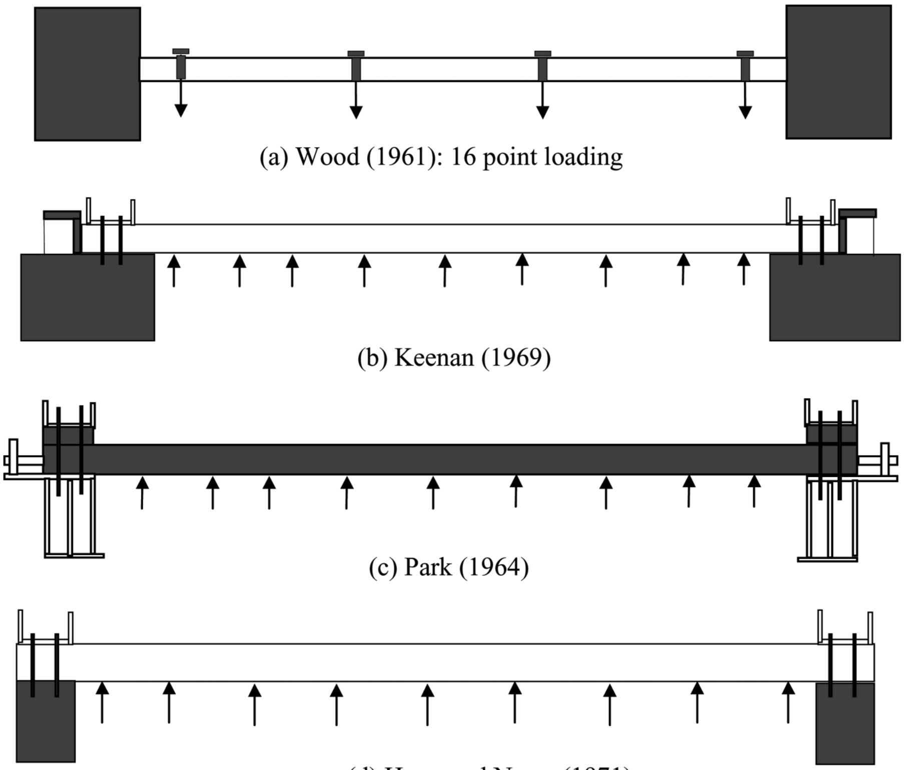
(a) Wood (1961): 16 point loading

(b) Keenan (1969)

(c) Park (1964)

(d) Hung and Nawy (1971)

Fig. 1 Laboratory representation of fully restrained edge conditions and uniformly distributed loading by different authors

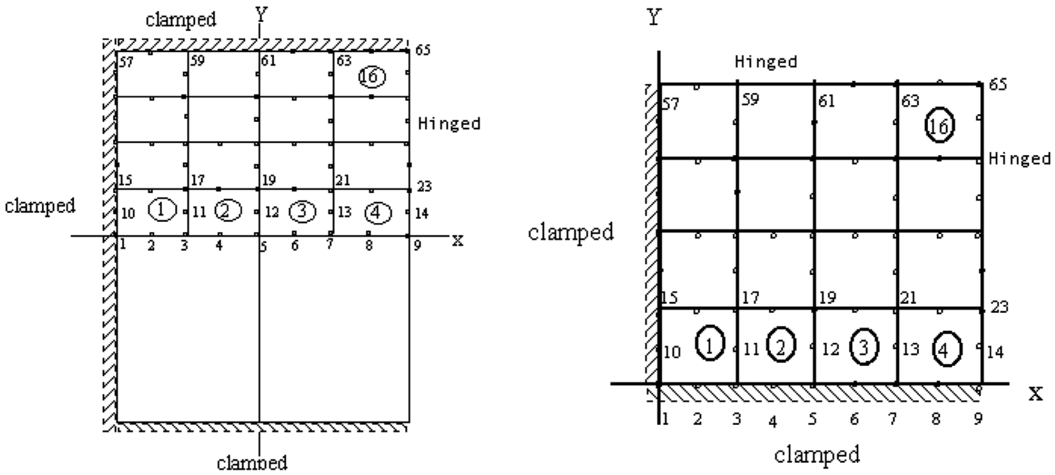

(a) Class II slabs (Hossain and Famiyesin 2001)

(b) Class III slabs (Hossain and Famiyesin 1998)

Fig. 2 Finite element mesh for partially clamped slabs translational and two rotational degrees of freedom (see Owen and Figueiras 1984). The material model comprises of a work-hardening plasticity based yield criterion, described by a modified Drucker Prager surface, which has a curved meridian, and is expressed in terms of the stress components as:

$$f(\sigma) = 2\{1.355[(\sigma_x^2 + \sigma_y^2 - \sigma_x\sigma_y) + 3(\tau_{xy}^2 + \tau_{xz}^2 + \tau_{yz}^2)] + 0.355\sigma_o(\sigma_x + \sigma_y)\}^{0.5} = \sigma_0 \qquad (1)$$

where σ_o is the equivalent effective stress, which for the work hardening model, is taken as $0.3f'_c$, where f'_c is the uniaxial compressive strength of concrete. The crushing condition is expressed in terms of strain components as:

$$1.355[(\varepsilon_x^2 + \varepsilon_y^2 - \varepsilon_x\varepsilon_y) + 0.75(\gamma_{xy}^2 + \gamma_{xz}^2 + \gamma_{yz}^2)] + 0.355\varepsilon_{cu}(\varepsilon_x + \varepsilon_y) = \varepsilon_{cu}^2 \qquad (2)$$

where ε_{cu} is the ultimate compressive strain in concrete which, when reached signifies the loss of all strength and rigidity.

A linear elastic response is assumed for concrete under tensile stresses until the fracture surface is reached, governed by a maximum tensile strength criterion (tension cut-off). Cracks are assumed to form in planes perpendicular to the direction of maximum principal tensile stress as soon as this reaches the specified concrete tensile strength f_t'. Tension stiffening is represented by a gradual post-peak stress release for the stress component normal to the cracked plane. The crack is assumed to be fully opened when a specified strain value (typically 0.002 is reached). An elastoplastic Von Mises idealisation is adopted to model the reinforcement as in Owen and Figueiras (1984). The model has been implemented into the Fortran program CONSHELL (Owen and Figueiras 1984) which was used in the basic simulations and subsequent database development.

3. Finite element simulations and predictions

3.1 RC slab simulations

As indicated above the primary field of application considered in this paper are partially restrained RC slabs under uniformly distributed loading, referred to as classes II and III slabs in Hossain and Famiyesin (2001). Representative of the class II partially restrained slabs are the four series C slabs tested by Park (1964) whose details are as shown in Table 1. The three-dimensional degenerated shell elements are used to discretize the symmetric half of the slab into 16 parabolic finite elements (Fig. 2a), with 10 layers taken through the depth. The four Park's slabs, whose three edges are restrained as in Fig. 1(c) were involved in the basic simulation process which has been fully reported in Famiyesin and Hossain (1998b). The simulation process established a FE-model for this class of problem, which in load-controlled analyses gave the ratios of the experimental-to-FE-predicted limit-loads, from between 0.83 to 1.05 for the four slabs, averaging at 0.95. In these series C slabs, (referred to hereafter as class II^{A}), one long edge is hinged while the other three edges are fixed, and in the series B slabs, (also tested by Park 1964 and involving three edges fixed as in Fig. 1c), one short edge is hinged. Details of the series B slabs (which will be referred to as class II^{B}) are also shown in Table 1 and will be used later for comparison. Other experimental slabs categorised under class II are cases where the three restrained edges were modelled as in Fig. 1(d).

Table 1 Details of classes **II^A** (series C) and **II^B** (series B) slabs tested by Park (1964) (1524 × 1016 × 50.8 mm)[(a)]

Slab No.	Aspect ratio a	Width-to-depth $L_x/h = b$	% of Steel				f_y N/mm^2	f_c'
			Short span		Long span			
			Top	Bottom	Top	Bottom		
C Series (**II^A**): 3 edges fully restrained (Fig. 1c) and one **long** edge simply supported								
C1	1.50	20	0.38	0.19	0.41	0.20	327.6	34.5
C2	1.50	20	0.84	0.42	0.43	0.21	327.6	30.2
C3	1.50	20	1.44	0.72	0.45	0.22	327.6	28.0
C4	1.50	20	2.42	1.21	0.47	0.23	327.6	35.1
B Series (**II^B**): 3 edges fully restrained (Fig. 1c) and one **short** edge simply supported								
B1	1.50	20	0.38	0.19	0.41	0.20	327.6	24.6
B2	1.50	20	0.84	0.42	0.43	0.21	327.6	24.9
B3	1.50	20	1.44	0.72	0.45	0.22	327.6	25.8
B4	1.50	20	2.42	1.21	0.47	0.23	327.6	26.0

Note[(a)] L_x: width of slab; h: overall depth of slab; f_y: steel yield strength; f'_c: concrete cylinder strength

Table 2 Details of classes **II^C** and **II^D** partially restrained slabs (3 edges fully restrained as in Fig. 1(d) and one long edge hinged)

Slab No.	Aspect ratio ***a*** L_y/L_x	Width-to-depth ***b*** L_x/h	Effective depth d, mm	% Steel	f_y N/mm^2	f_c' N/mm^2
II^C - Hung & Nawy (1971) - (1651 × 1651 × 63.5 mm)						
C2-1	1.0	26	50.8	0.58	471.0	38.6
C2-2	1.0	26	50.8	0.28	471.0	38.6
C2-3	1.0	26	50.8	0.36	475.2	41.9
C2-4	1.0	26	50.8	0.38	471.0	41.9
C2-5	1.0	26	50.8	0.58	286.9	39.0
II^C - Hung & Nawy (1971) - (1651 × 1194 × 63.5 mm)						
C5-1	1.38	18.8	50.8	0.36	475.2	27.1
C5-2	1.38	18.8	50.8	0.28	471.0	27.1
C5-3	1.38	18.8	50.8	0.58	471.0	34.1
C5-4	1.38	18.8	50.8	0.58	286.9	34.1
II^D - Nawy & Blair (1971) - (1524 × 1524 × 63.5 mm)						
WV8	1.0	24	50.8	0.575	480.27	39.31
WV9	1.0	24	50.8	0.288	480.27	39.31
WV10	1.0	24	50.8	0.477	484.5	42.75
WV11	1.0	24	50.8	0.383	480.27	42.75
WV12	1.0	24	50.8	0.579	480.27	39.8
II^D - Nawy & Blair (1971) - (1524 × 1066.8 × 63.5 mm)						
WV30	1.43	16.8	50.8	0.358	484.5	27.64
WV31	1.43	16.8	50.8	0.288	480.27	27.64
WV32	1.43	16.8	50.8	0.575	480.27	34.81
WV33	1.43	16.8	50.8	0.579	292.52	34.81

These are the nine slabs (C2-1 to C2-5 and C5-1 to C5-4) tested by Hung and Nawy (1971) and referred to as class II^C, and the nine slabs (WV8-WV12 and WV30-WV33) tested by Nawy and Blair (1971) and referred to as class II^D. Details of these slabs are summarised in Table 2.

In the class III ‘partially restrained slabs’, adjacent slab edges are fully restrained and the other adjacent edges are hinged. Representative of this class are the eight slabs (C3-1 to C3-5 and C6-1 to C6-3), tested by Hung and Nawy (1971) and referred to as class III^C and the eight slabs (WV13-WV17 and WV34-WV36), tested by Nawy and Blair (1971) and referred to as class III^D. The details of these slabs are summarised in Table 3 and the restrained edges are as shown in Fig. 1(d). The basic simulation process used for establishing a reliable FE model for class III slabs involved the three series C6 slabs of Table 3 which are discretized into sixteen finite elements as shown in Fig. 2(b). Their analyses using a load-controlled strategy, gave the ratios of experimental-to-FE predicted limit loads for the three slabs, to vary from 0.97-1.024 and averaging at 1.00, as reported by Hossain and Famiyesin (1998).

Some class I RC slabs (where all the four edges are ‘fully restrained’), have been tested by Hung and Nawy (1971), with the edge conditions represented as in Fig. 1(d) having no lateral restraints.

Table 3 Details of classes **III^C** and **III^D** slabs (adjacent edges restrained as in Fig. 1(d) and adjacent edges hinged)

Slab No.	Aspect ratio ***a*** L_y/L_x	Width-to-depth ***b*** L_x/h	Effective depth *d*, mm	% Steel	f_y N/mm^2	f_c' N/mm^2
			III^C - Hung & Nawy (1971) - (1651 × 1194 × 63.5 mm)			
C6-1	1.38	18.8	50.8	0.28	471.0	29.8
C6-2	1.38	18.8	50.8	0.36	475.0	29.8
C6-3	1.38	18.8	50.8	0.58	286.9	30.0
			III^C - Hung & Nawy (1971) - (1651 × 1651 × 63.5 mm)			
C3-1	1.0	26	50.8	0.36	286.9	28.3
C3-2	1.0	26	50.8	0.28	471.0	28.3
C3-3	1.0	26	50.8	0.58	471.0	35.9
C3-4	1.0	26	50.8	0.58	471.0	35.2
C3-5	1.0	26	50.8	0.58	475.2	33.0
			III^D - Nawy & Blair (1971) - (1524 × 1524 × 63.5 mm)			
WV13	1.0	24	50.8	0.579	292.52	28.83
WV14	1.0	24	50.8	0.575	480.27	28.83
WV15	1.0	24	50.8	0.288	480.27	36.57
WV16	1.0	24	50.8	0.383	480.27	36.57
WV17	1.0	24	50.8	0.358	484.5	33.61
			III^D - Nawy & Blair (1971) - (1524 × 1066.8 × 63.5 mm)			
WV34	1.43	16.8	50.8	0.288	480.27	30.38
WV35	1.43	16.8	50.8	0.358	484.5	30.38
WV36	1.43	16.8	50.8	0.579	292.52	30.59

Table 4 Details of class **I**$^{\mathbf{C}}$ slabs, all edges fully restrained as in Fig. 1(d); Hung & Nawy (1971)

Slab No.	Aspect ratio ***a*** L_y/L_x	Width-to-depth ***b*** L_x/h	Effective depth *d*, mm	% Steel	f_y N/mm^2	f'_c N/mm^2
I$^{\mathbf{C}}$ - Slab dimensions: $1651 \times 1651 \times 63.5$ mm						
C1-1	1.0	26	50.8	0.58	471.0	38.6
C1-2	1.0	26	50.8	0.36	475.2	38.6
C1-3	1.0	26	50.8	0.28	471.0	33.1
C1-4	1.0	26	50.8	0.25	474.5	38.6
C1-5	1.0	26	50.8	0.36	475.2	34.4
C1-6	1.0	26	50.8	0.38	471.0	34.4
C1-7	1.0	26	50.8	0.58	286.9	39.0
I$^{\mathbf{C}}$ - Slab dimensions: $1651 \times 1194 \times 63.5$ mm						
C4-1	1.38	18.8	50.8	0.58	286.9	33.0
C4-2	1.38	18.8	50.8	0.28	471.0	39.8
C4-3	1.38	18.8	50.8	0.58	471.0	39.8
C4-4	1.38	18.8	50.8	0.36	475.2	34.6
C4-5	1.38	18.8	50.8	0.38	471.0	34.6

Table 5 Details of class **I**$^{\mathbf{A}}$ slabs, all edges fully restrained as in Fig. 1(c); Park (1964): $1524 \times 1016 \times 50.8$ mm

Slab No.	Aspect ratio ***a***	Width-to-depth L_x/h = ***b***	% of Steel				f_y N/mm^2	f'_c N/mm^2
			Short span		Long span			
			Top	Bottom	Top	Bottom		
A1	1.50	20	0.38	0.19	0.41	0.20	327.6	33.0
A2	1.50	20	0.84	0.42	0.43	0.21	327.6	29.5
A3	1.50	20	1.44	0.72	0.45	0.22	327.6	34.4
A4	1.50	20	2.42	1.21	0.47	0.23	327.6	27.7

The slabs tested were C1-1 to C1-7 and C4-1 to C4-5, whose details are shown in Table 4. With the absence of lateral restraints, rotation at the slab edges cannot be totally prevented hence the slabs are effectively partially restrained. The ability of the equations, (derived on the basis of class II^{A}-Park's series C type of slabs), to predict the limit loads of such class I slab is also investigated in this paper. Details of other class I slabs restrained laterally as in Fig. 1(c), which have been tested by Park (1964) and shown in Table 5, are also included to give further insight into the limitations of the developed equations.

3.2 RC slab predictions

With the two FE models established in the previous section for the partially restrained classes II and III RC slabs, analyses of many 'numerical model' slabs with different material and geometric parameters were then carried out. These provide a database of peak loads that forms the basis for the equation development process, which will be described in the next section. The relevant slab parameters varied include the aspect ratio, the width-to-depth ratio, the steel reinforcement ratio (in

Table 6 Parameters used for the analysis of computer-model RC slabs

Aspect ratio ***a***	Width to depth ratio ***b***	Cylinder[a] strength, f'_c	Steel yield[a] strength, f_y	Steel ratio ρ (%)
2.0	15	25	250	0.2
1.5	20	40	460	0.5
1.0	25	60	-	1.0
-	30	-	-	-
-	35	-	-	-

Note[(a)] Units in N/mm^2

%), the concrete cylinder strength and the steel yield stress. Table 6 shows the parameters used for the analysis of the different types of partially restrained slabs. 270 FE analyses each were carried out for class II slabs (for the cases where one long edge or one short edge is hinged, while the other three edges are fully restrained). 270 FE analyses were also carried out for class III slabs where a pair of adjacent edges is fully restrained and the other pair is hinged, (or simply supported) as shown in Fig. 2(b). A total of 810 FE analyses resulted from the study and each slab was assumed to be isotropically reinforced at the top (for clamped edges) and bottom, and the cover to reinforcement is assumed to be 20% of the slab thickness. The load is uniformly distributed over the surface of the slabs and applied in increments during the analysis. The percentage of steel is calculated on the basis of the mean effective depth of the slab. The FE discretisation adopted is similar to those described earlier for the basic FE simulation process. Full details of the analyses carried out for the database development are contained in Hossain and Famiyesin (1998) and Famiyesin and Hossain (1998b). The process of equation development from the database of results obtained from the 270 FE analyses of class II^A slabs, (where one long edge is hinged and 3 edges are restrained as in Fig. 1c), is discussed in this paper. The effectiveness and limitations of the developed equations for limit load prediction resulting from this data-set, is illustrated by their use for partially restrained slabs of similar description (class II^A), and other slabs with different partial restraints (classes II^B, II^C, II^D, III^C and III^D). Some 'fully restrained' class I slabs whose boundary condition is similar to Fig. 1(d) are also used to test the limitation of the developed equations.

4. Process of equation development

Three equations for the limit load prediction of partially restrained slabs are developed in this section, employing two main procedures. The first procedure adopts a two-stage approach by defining normalised parameters of slab geometry and material properties, and relating these to the relevant limit loads in the database. The whole RC slab problem is treated as a combination of subsystems. At the first stage linear relationships are established at the subsystem level between two normalised parameters, resulting in sets of gradients and intercepts of their 'lines of best fit'. The second stage involves relating each of these sets of gradients and intercepts to different combinations of the slab geometry parameters; the aspect ratio a and the width-to-depth ratio b. Two limit load equations were developed by this two-stage approach referred to respectively as $\boldsymbol{w_{p1}}$ and $\boldsymbol{w_{p2}}$. The second procedure uses the MATLAB software to develop the third limit-load equation, which directly relates the limit load ($\boldsymbol{w_{p3}}$) to all slab parameters.

4.1 Method 1: Normalised equation for RC slabs (w_{p1} and w_{p2})

Following the FE analyses of the 270 numerical-model RC slabs with partial restraints (of class II^A description), the database of peak loads obtained are used in setting up two, non-dimensional parameters α and β which are defined as:

$$\alpha = \frac{\text{Peak load}}{\text{Concrete cube strength}} = \frac{w_p}{f_{cu}} \tag{3}$$

and

$$\beta = \frac{\text{steel yield strength}}{\text{Concrete cube strength}} \times \text{Steel percentage} = \frac{f_y}{f_{cu}} \times \rho \tag{4}$$

where w_p is the peak load obtained from the FE analysis but will later be defined as the predicted limit load, ρ is the steel ratio (in %), f_y is the steel yield stress, and the concrete cube strength f_{cu} (which conforms to the British code of practice, BS8110 1985), is assumed to be related to the cylinder strength f_c' (conforming to ACI code, 1989) as:

$$f_c' \cong 0.8 f_{cu} \tag{5}$$

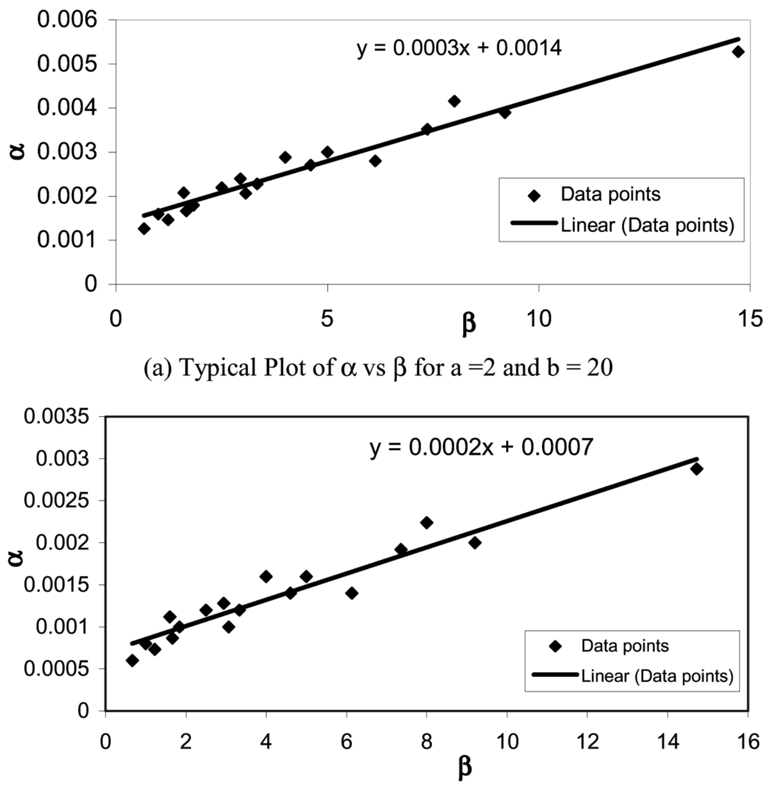

(a) Typical Plot of α vs β for a =2 and b = 20

(b) Typical Plot of α vs β for a =1.5 and b = 30

Fig. 3 Variation of normalised parameter α vs β

The parameter α is a function of parameter β, the aspect ratio a and the width-to-depth ratio b such that

$$\alpha = F(\beta, a, b) \tag{6}$$

The nature of the above function has been established by plotting α against β for various combinations of a and b for each class of slabs from Table 6, which results in fifteen combinations and hence fifteen plots. Typical normalised plots for the class II^{A} slabs are shown in Figs. 3(a & b). In the plots, linear relationships are established of the form:

$$\alpha = I + M\beta \tag{7}$$

where I is the intercept and M is the gradient of the 'line of best fit', which are themselves functions of the aspect ratio a and the width-to-depth ratio b. The values of I and M for the fifteen combinations of a and b were noted and their individual variation with a and b were established as:

$$I = P\, a^{u} b^{v} + C_1 \quad \text{and} \quad M = Q\, a^{y} b^{z} + C_2 \tag{8}$$

where P, Q, u, v, y, z, C_1 and C_2 are suitable constants to be determined. Suitable expressions established for the variation of both I and M using the fifteen combinations of a and b for the partially restrained class II slabs (shown in Figs. 4(a & b)), are:

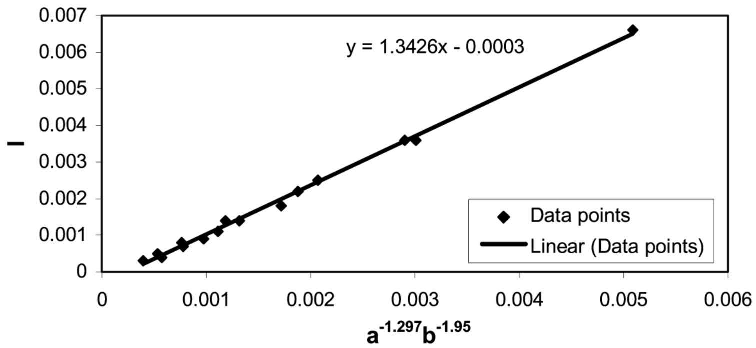

(a) Plot of ***I*** vs $\boldsymbol{a}^{-1.297}\,\boldsymbol{b}^{-1.95}$

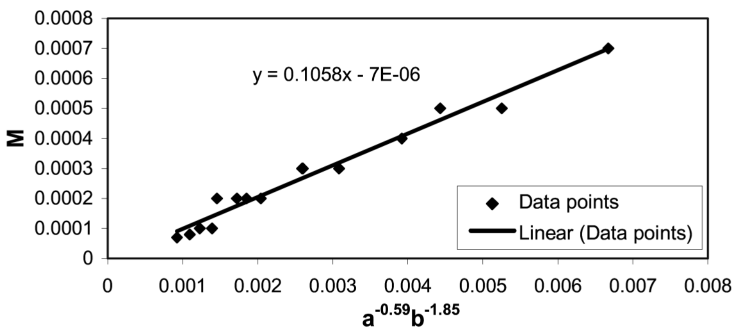

(b) Plot of ***M*** vs $\boldsymbol{a}^{-0.59}\,\boldsymbol{b}^{-1.85}$

Fig. 4 Relationship of ***I*** and ***M*** with combinations of ***a*** and ***b***

$$I = 1.3426a^{-1.297}b^{-1.95} - 0.0003 \tag{9}$$

and
$$M = 0.1058a^{-0.59}b^{-1.85} - 0.000007 \tag{10}$$

Therefore the final expression for the normalised parameter α can be assembled from Eqs. (3, 7, 9 & 10) as:

$$\alpha = [(1.3426a^{-1.297}b^{-1.95} - 0.0003) + (0.1058a^{-0.59}b^{-1.85} - 0.000007)\ \beta]$$

and the predicted peak load $\boldsymbol{w_{p1}}$ from Eq. (3) is defined as

$$w_{p1} = f_{cu}[(1.3426a^{-1.297}b^{-1.95} - 0.0003) + (0.1058a^{-0.59}b^{-1.85} + 0.000007)\ \beta] \tag{11}$$

The second equation is obtained by using other suitable constants to define I and M as:

$$I = 1.4a^{-1.297}b^{-1.95} - 0.0005 \tag{12}$$

and
$$M = 0.1024a^{-0.59}b^{-1.85} - 0.00003 \tag{13}$$

from which we arrive at the final equation $\boldsymbol{w_{p2}}$ defined as:

$$w_{p2} = f_{cu}[(1.4a^{-1.297}b^{-1.95} - 0.0005) + (0.1024a^{-0.59}b^{-1.85} + 0.00003)\beta] \tag{14}$$

4.2 Method 2: Matlab generated equation for RC slabs (w_{p3})

The basic parameters associated with RC slabs are the aspect ratio (a), width-to-depth ratio (b), concrete cylinder strength (f'_c), reinforcement yield stress (f_y) and reinforcement ratio ρ(%). The reinforcement ratio ρ is defined as $A_s/L_x d \times 100\%$, where A_s is the cross sectional area of the slabs main reinforcement, L_x is the width of the slab and d is the effective depth.

With these basic parameters a general relationship may be formed with the limit load prediction equation as:

$$w_{p3} = A.a^B b^C f_c'^D f_y^E \rho^F \tag{15}$$

where A, B, C, D, E and F are constants that are identified by the Matlab software (Herniter 2001). Eq. (15) is expressed in logarithmic format to transform it into a linear relationship, (which makes the identification of the equation constants easier within Matlab), as:

$$\log(w_{p3}) = \log A. + B\log(a) + C\log(b) + D\log(f_c') + E\log(f_y) + F\log(\rho) \tag{16}$$

The database of the 270 class II slab results were used with Eq. (16) in Matlab to identify the various constants as; $A = 10^{1.1647}$; $B = -1.0896$; $C = -2.2332$; $D = 0.2918$; $E = 0.3041$ and $F = 0.4427$; such that the final limit load prediction equation becomes:

$$w_{p3} = 10^{1.1647} a^{-1.0896} b^{-2.2332} f_c'^{0.2918} f_y^{0.3041} \rho^{0.4427} \tag{17}$$

5. Verification of the developed equations

Partially restrained RC slabs have been defined in this paper as those belonging to classes II and III. The RC slabs in class II are rectangular slabs which have three of their edges fully restrained, and the fourth long (or short) edge hinged. Belonging to this class are the following groups of slabs tested by different authors:

- Slabs (C1-C4) tested by Park (1964) where one long edge is hinged and three edges are clamped as in Fig. 1(c). This group of slabs is referred to as class $\mathbf{II^A}$ and its database of FE results has been used to develop the peak load-prediction Eqs. (11), (14) and (17).
- Slabs (B1-B4) tested by Park (1964) where one short edge is hinged and the fixed edges are interpreted as in Fig. 1(c). This group is referred to as class $\mathbf{II^B}$ and is stiffer than the class $\mathbf{II^A}$ slabs.
- Slabs (C2-1 to C2-5 and C5-1 to C5-4) tested by Hung and Nawy (1971) where one long edge is hinged and the fixed edges are interpreted as in Fig. 1(d)-(referred to as class $\mathbf{II^C}$)
- Slabs (WV8-WV12 and WV30-WV33) tested by Nawy and Blair (1971) where one long edge is hinged and the fixed edges are interpreted as in Fig. 1(d)-(referred to as class $\mathbf{II^D}$). This group is created different from class $\mathbf{II^C}$ in order to assess the effect of different author's implementation of the same set of boundary conditions.

RC slabs in Class III have two adjacent edges fully restrained and two adjacent edges hinged. Again, as in the class II slabs the class III RC slabs have been tested by different authors and are identified uniquely in this paper on the basis of the author who carried out the tests. The reasons for this will become evident in the next few paragraphs. The class III slabs tested are grouped as follow:

- Slabs (C3-1 to C3-5 and C6-1 to C6-3) tested by Hung and Nawy (1971) with the restrained edges as in Fig. 1(d)-(referred to class $\mathbf{III^C}$).
- Slabs (WV13-WV17 and WV34-WV36) tested by Nawy and Blair (1971) with the restrained edges as in Fig. 1(d)-(referred to class $\mathbf{III^D}$).

The effectiveness of the equation prediction for class I slabs, (where all the four edges are fully restrained to varying degrees), will be assessed with the following two groups of experimental tests:

- Slabs (A1-A4) tested by Park (1964) where all the edges are restrained as in Fig. 1(c)-(class $\mathbf{I^A}$).
- Slabs (C1-1 to C1-7 and C4-1 to C4-5) tested by Hung and Nawy (1971) with the restrained edges as in Fig. 1(d)-(class $\mathbf{I^C}$).

Out of 810 FE analyses carried out for three different types of partially restrained RC slabs (under classes II and III), only the 270 results relating to the class $\mathbf{II^A}$ slabs, (where three edges are fixed as in Fig. 1c), have been used to derive the prediction Eqs. (11), (14) and (17). However, the ability of the derived equations to predict the peak load for other types of slabs, (such as those in classes $\mathbf{I^A}$, $\mathbf{I^C}$, $\mathbf{II^B}$, $\mathbf{II^C}$, $\mathbf{II^D}$, $\mathbf{III^C}$ and $\mathbf{III^D}$), is also considered in this paper. If desired, equations specific to classes $\mathbf{II^B}$ and $\mathbf{III^C}$ slab categories may be developed from the rest of the database using the procedures similar to the ones outlined above.

5.1 Verification of equations for partially restrained RC slabs

In order to verify Eqs. (11), (14) and (17), developed on the basis of class $\mathbf{II^A}$ for predicting the peak loads of partially restrained slabs, comparison with previous experimental tests is now carried out. For class II slabs, Tables 7 and 8 show the ratios of experimental-to-predicted loads for 26 slabs using the three equations developed. Table 9 uses the same set of equations to predict the limit loads for 16 class III slabs while Tables 10 and 11 show the predictions for 16 slabs in class I. Three authors, Park (1964), Hung and Nawy (1971) and Nawy and Blair (1971) have tested all

Table 7 Comparison of predicted and experimental limit loads (classes $\mathbf{II^A}$, $\mathbf{II^C}$ and $\mathbf{II^D}$) slabs

Slab type	**Experiment *w*** 10^3 (kN/m^2)	**Ratios of experimental-to-predicted loads**		
		'Best fit' FE Eq. (11) w/w_{p1}	'Best fit' FE Eq. (14) w/w_{p2}	MATLAB Eq. (17) w/w_{p3}
Park's Slabs (1964) - Series C - $\mathbf{II^A}$				
C1	0.115	1.082	1.152	1.256
C2	0.130	1.087	1.169	1.039
C3	0.125	0.859	0.933	0.804
C4	0.183	0.853	0.930	0.876
Hung and Nawy (1971) - $\mathbf{II^C}$				
C2-1	0.14	0.813	0.884	0.900
C2-2	0.11	0.832	0.893	1.004
C2-3	0.13	0.858	0.924	1.027
C2-4	0.15	0.959	1.033	1.139
C2-5	0.13	0.953	1.026	1.036
C5-1	0.14	0.933	0.989	0.893
C5-2	0.13	0.946	0.999	0.916
C5-3	0.20	0.938	0.998	0.955
C5-4	0.18	1.040	1.098	0.999
Nawy and Blair (1971) - $\mathbf{II^D}$				
WV8	0.1377	0.689	0.737	0.760
WV9	0.113	0.707	0.748	0.847
WV10	0.1303	0.661	0.704	0.761
WV11	0.1494	0.816	0.865	0.966
WV12	0.1367	0.678	0.726	0.751
WV30	0.143	0.759	0.794	0.716
WV31	0.1323	0.770	0.803	0.734
WV32	0.2012	0.765	0.804	0.768
WV33	0.1828	0.852	0.888	0.808
Average Ratio		**0.857**	**0.914**	**0.907**
Standard Deviation		**0.125**	**0.135**	**0.1424**

Table 8 Ability of equations to predict limit loads for other class **II**^{B} slabs - one short edge hinged/simply supported and three edges fully fixed

Slab type	**Experiment *w*** 10^3 (kN/m^2)	**Ratios of experimental-to-predicted loads**		
		'Best fit' FE Eq. (11) w/w_{p1}	'Best fit' FE Eq. (14) w/w_{p2}	MATLAB Eq. (17) w/w_{p3}
Park's Slabs (1964) - Series B - **II**^{B}				
B1	0.140	1.718	1.835	1.688
B2	0.167	1.571	1.694	1.412
B3	0.180	1.286	1.398	1.186
B4	0.230	1.200	1.313	1.202
Average Ratio		**1.443**	**1.560**	**1.372**
Standard Deviation		**0.242**	**0.246**	**0.234**

Table 9 Ability of equations to predict limit loads for classes **III**^{C} and **III**^{D} slabs - adjacent edges fully fixed, adjacent edges hinged

Slab type	**Experiment *w*** 10^3 (kN/m^2)	**Ratios of experimental-to-predicted loads**		
		'Best fit' FE Eq. (11) w/w_{p1}	'Best fit' FE Eq. (14) w/w_{p2}	MATLAB Eq. (17) w/w_{p3}
Hung and Nawy (1971) - **III**^{C}				
C6-1	0.1212	0.830	0.874	0.831
C6-2	0.1249	0.776	0.822	0.764
C6-3	0.163	1.020	1.079	0.939
C3-1	0.125	1.279	1.374	1.311
C3-2	0.142	1.355	1.462	1.431
C3-3	0.113	0.710	0.773	0.770
C3-4	0.122	0.775	0.844	0.836
C3-5	0.11	0.722	0.787	0.766
Nawy and Blair (1971) - **III**^{D}				
WV13	0.127	0.930	0.992	0.892
WV14	0.1449	0.865	0.932	0.878
WV15	0.1152	0.762	0.806	0.885
WV16	0.125	0.761	0.809	0.846
WV17	0.1117	0.733	0.780	0.796
WV34	0.1236	0.677	0.705	0.667
WV35	0.1272	0.640	0.669	0.621
WV36	0.1663	0.841	0.878	0.764
Average Ratio		**0.855**	**0.912**	**0.875**
Standard Deviation		**0.204**	**0.222**	**0.211**

the experimental slabs considered in this paper. The tests carried out by Hung and Nawy and by Nawy and Blair, were done in groups. For instance in Table 7, Hung and Nawy (1971) carried out tests on two groups of slabs with class II configuration. These are the C2-1 to C2-5 and C5-1 to C5-4, which for ease of assessment have been separated with a horizontal line. Similar demarcation lines appear for the two authors in Tables 9 and 10 where such class grouping exists. What the tables reveal is that on average, there is general consistency in the ratios obtained for each author's tests. This supports the view that while each author's interpretation of 'full restraint'

Table 10 Ability of equations to predict limit loads for class $\mathbf{I^C}$ slabs - all edges fully restrained as in Fig. 1(d)

Slab type	**Experiment *w*** 10^3 (kN/m^2)	**Ratios of experimental-to-predicted loads**		
		'Best fit' FE Eq. (11) w/w_{p1}	'Best fit' FE Eq. (14) w/w_{p2}	MATLAB Eq. (17) w/w_{p3}
		Hung and Nawy (1971) - $\mathbf{I^C}$		
C1-1	0.16	0.963	1.047	1.067
C1-2	0.13	0.924	0.995	1.068
C1-3	0.1214	1.025	1.103	1.156
C1-4	0.1214	0.939	1.007	1.159
C1-5	0.133	0.993	1.073	1.098
C1-6	0.1397	1.058	1.144	1.162
C1-7	0.1611	1.138	1.226	1.237
C4-1	0.214	1.192	1.257	1.170
C4-2	0.19	0.995	1.043	1.166
C4-3	0.222	0.909	0.964	0.987
C4-4	0.21	1.121	1.182	1.198
C4-5	0.201	1.056	1.114	1.123
Average Ratio		**1.026**	**1.096**	**1.133**
Standard Deviation		**0.090**	**0.092**	**0.068**

Table 11 Ability of equations to predict limit loads for class $\mathbf{I^A}$ slabs - all edges fully restrained as in Fig. 1(c)

Slab type	**Experiment *w*** 10^3 (kN/m^2)	**Ratios of experimental-to-predicted loads**		
		'Best fit' FE Eq. (11) w/w_{p1}	'Best fit' FE Eq. (14) w/w_{p2}	MATLAB Eq. (17) w/w_{p3}
		Park (1964) - $\mathbf{I^A}$		
A1	0.22	2.145	2.285	2.434
A2	0.22	1.867	2.009	1.770
A3	0.26	1.610	1.742	1.576
A4	0.26	1.327	1.451	1.334
Average Ratio		**1.737**	**1.872**	**1.778**
Standard Deviation		**0.350**	**0.358**	**0.472**

Table 12 Summary of limit load predictions

Author/class/ slab details	No. of slabs	Ratios of experimental-to-predicted loads					
		w/w_{p1} - Eq. (11)		w/w_{p2} - Eq. (14)		w/w_{p3} - Eq. (17)	
		Range	Average	Range	Average	Range	Average
Park - $\mathbf{I}^{\mathbf{A}}$							
A1-A4	4	1.33-2.15	1.74	1.45-2.29	1.87	1.33-2.43	1.78
Hung & Nawy - $\mathbf{I}^{\mathbf{C}}$							
C1-1 to C1-7	7	0.94-1.14	1.01	1.00-1.23	1.09	1.07-1.24	1.14
C4-1 to C4-5	5	0.91-1.19	1.06	0.96-1.26	1.11	0.99-1.20	1.13
Park - $\mathbf{II}^{\mathbf{A}}$ **							
C1-C4	4	0.85-1.09	0.97	0.93-1.17	1.05	0.80-1.26	0.99
Park - $\mathbf{II}^{\mathbf{B}}$							
B1-B4	4	1.20-1.72	1.443	1.31-1.84	1.560	1.19-1.69	1.372
Hung & Nawy - $\mathbf{II}^{\mathbf{C}}$							
C2-1 to C2-5	5	0.81-0.96	0.88	0.88-1.03	0.95	0.9-1.14	1.02
C5-1 to C5-4	4	0.93-1.04	0.96	0.99-1.10	1.02	0.89-1.00	0.94
Nawy & Blair - $\mathbf{II}^{\mathbf{D}}$							
WV8-WV12	5	0.66-0.82	0.71	0.70-0.87	0.76	0.75-0.97	0.82
WV30-WV33	4	0.76-0.85	0.79	0.79-0.89	0.82	0.72-0.81	0.76
Hung & Nawy - $\mathbf{III}^{\mathbf{C}}$							
C3-1 to C3-5	5	0.71-1.36	0.97	0.77-1.46	1.05	0.77-1.43	1.02
C6-1 to C6-3	3	0.78-1.02	0.88	0.82-1.08	0.93	0.76-0.94	0.85
Nawy & Blair - $\mathbf{III}^{\mathbf{D}}$							
WV13-WV17	5	0.73-0.93	0.81	0.78-0.99	0.86	0.80-0.89	0.86
WV34-WV36	3	0.64-0.84	0.72	0.67-0.88	0.75	0.62-0.76	0.68

**Reference class for equations

may be different from the others, such an interpretation will be consistent for all the slabs tested by the author.

Table 12 gives an overall summary of the limit load prediction for each class of slabs on the basis of authors and test grouping. As would be expected the predictions for class II^A slabs, which was the subject group used for equation development, was very accurate, giving average ratio values of between 0.97 to 1.05. It would be recalled that for this particular group the three edges were restrained as in Fig. 1(c). Relative to this group other slabs in class II were either less or more flexible depending on how many slab edges were restrained and whether lateral restraint (as in Fig. 1c) was present or not at the restrained edges. In class II^B slabs, where one short edge is hinged and the other three edges were restrained in a way similar to II^A, a stiffer response (as expected) is reported as indicated by the higher average ratios. For classes II^C and II^D slabs, which were restrained as in Fig. 1(d), a more flexible response than II^A is noted (by the lower average ratios). For tests carried out on slabs belonging to classes II^C and II^D, it is noted that while the boundary conditions may have been interpreted the same way, their actual physical implementation may have been different, as evidenced by the stiffer response for II^C slabs (Table 7). The consistency of the ratios within the group of slabs tested by each author, (Tables 7-12), which are different from other authors support this idea. Hung and Nawy's (1971) slabs (II^C) are noted to be consistently stiffer than Nawy and Blair's (1971) tests (II^D). This scenario is also repeated in the tests carried out by the two authors on class III slabs (compare III^C with III^D in Tables 9 and 12).

The ability of the developed equation to predict the limit loads of the stiffer slabs in class I is illustrated in Tables 10-12. For such group of slabs where all the edges are laterally restrained as in Fig. 1(c), (e.g., class I^A, tested by Park 1964), a very high experimental-to-predicted limit load ratios, ranging between 1.7 and 1.9, is recorded (see Table 11). However for the less stiff Hung and Nawy's class I^C slabs shown in Table 10, average ratios of about 1.10, which are only marginally higher than the reference predictions (II^A), are noted. Irrespective of whether the slab group under consideration is stiffer or more flexible than the reference group, the low standard deviation within the group shows a low level of scatter, thereby supporting the above stated theory of author-consistency in testing. Allowing for errors that are normally associated with experimental tests, and considering the low level of scatter noted for predictions within each slab group, it would seem that there is considerable potential in applying the methods outlined for RC slabs to other engineering problems.

It should be noted that the FE models used to generate the database of results have assumed rigid fixity to idealise clamped edges, with no rotation or displacement allowed. However authors who carry out physical tests on slabs with clamped edges interpret this fixity in different ways (Figs. 1(a-d)), such that while the test set-up largely does not allow displacement at such edges, rotations cannot be totally eliminated but do occur to varying degrees.

Figs. 5-7 show the comparison of the experimental results, from some of the tests considered above, with their corresponding predictions by the w_{p2} equation (i.e., Eq. 14). From these figures it can be noted that the experimental interpretation of fixity by Nawy and Blair (1971) is furthest from the idealised FE modelling, upon which the equations were based.

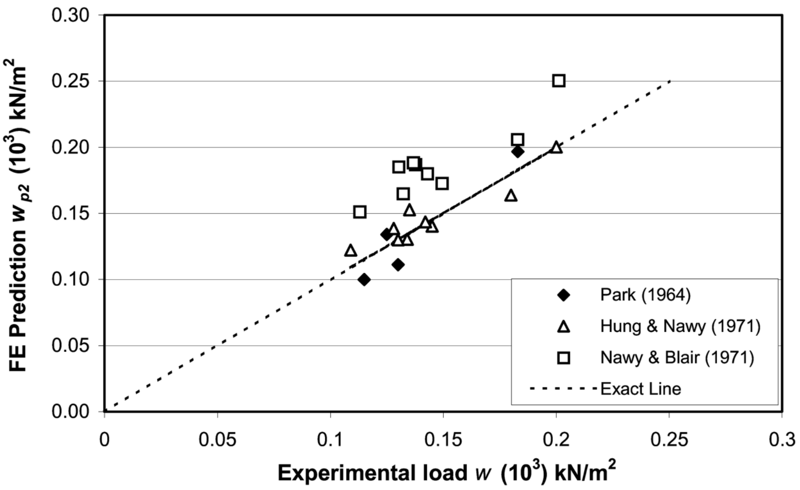

Fig. 5 Comparison of test results with FE equation predictions for class II slabs

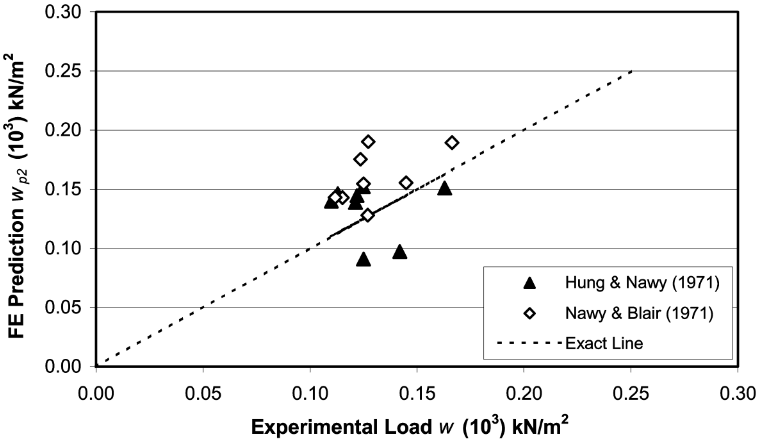

Fig. 6 Comparison of test results with FE equation predictions for class III slabs

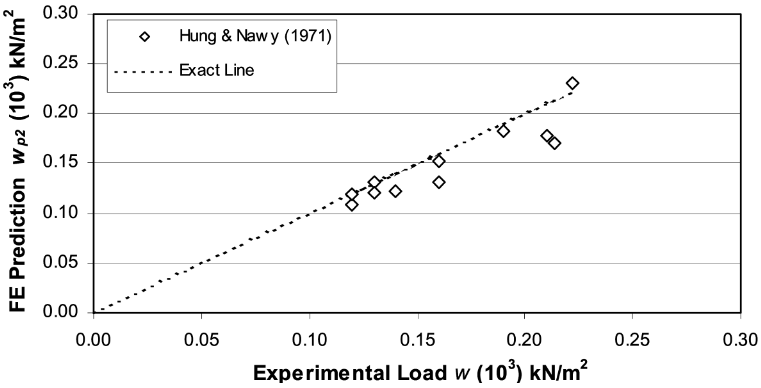

Fig. 7 Comparison of test results with FE equation predictions for class $\mathbf{I}^{C}$ slabs

6. Conclusions

Three equations for predicting the limit loads of partially restrained slabs, under uniformly distributed loading, have been developed from the database of peak loads generated by extensive FE analyses of partially restrained model RC slabs. The FE analyses of the 270 ‘numerical model’ class II^{A} slabs, used for the development of the prediction equations, covered a wide range of material and geometric parameters. The validity of the developed limit load equations for different classes of slabs has been demonstrated by comparing their predictions with available experimental data from different authors.

The proposed equations are simple to develop and are suitable for reinforced concrete slabs of different geometry and material parameters, within the classes of application. However, depending on which class is being considered, appropriate ratio factor should be used to guarantee exact prediction. The equations could also be easily coded on computers or evaluated by hand calculation without requiring expertise in FE analysis. They are therefore very useful for design assistance and could be of benefit to practising engineers, especially in cases where specific guidance has not been given in the relevant design codes. While the field of application for the developed equations has focused on partially restrained RC slabs, the consistency of the predictions reported for other classes of slabs, (and their low level of scatter), would tend to suggest that the methods outlined could be applied to other engineering problems.

References

ACI 318-89. (1989), “Building code requirements for reinforced concrete”, ACI Committee 318, American Concrete Institute, Detroit.

BS8110 (1985), “Structural use of concrete, Part 1. Code of practice for design and construction”, British Standard Institute, London.

Famiyesin, O.O.R. and Hossain, K.M.A. (1998a), “Optimised design charts for fully restrained slabs by FE predictions”, *J. Struct. Engrg.*, ASCE, **124**(5), 560-569.

Famiyesin, O.O.R. and Hossain, K.M.A. (1998b), “Development of charts for partially clamped slabs by FE predictions”, *J. Struct. Engrg.*, ASCE, **124**(11), 1339-1349.

Herniter, M.E. (2001), *Programming in MATLAB*, Brookes/Cole - Thomson Learning, California.

Hossain, K.M.A. and Famiyesin, O.O.R. (1997), “Design charts for simply supported concrete slabs based on finite element procedures”, *Proc., 5th Int. Conf. on Computational Plasticity* (COMPLAS), Barcelona, 1508-1513.

Hossain, K.M.A. and Famiyesin, O.O.R. (1998), “Application of finite element modelling to the design of partially clamped slabs”, *Proc., Australasian Structural Engineering Conf.*, Auckland, New Zealand, **1**, 281-288.

Hossain, K.M.A. and Famiyesin, O.O.R. (2001), “An intelligent system for the design of RC slabs”, *Struct. Eng. Mech.*, **12**(3), 297-312.

Hung, T.Y. and Nawy, E.G. (1971), “Limit strength and serviceability factors in uniformly loaded, iso-tropically reinforced two way slabs”, ACI SP-30, American Concrete Institute, Detroit, Mich., 301-324.

Keenan, W.A. (1969), “Strength and behaviour of restrained reinforced concrete slabs under static and dynamic loading”, Technical Report R621, U.S. Naval Civil Engineering Laboratory, Port Hueneme, California, April.

Nawy, E.G. and Blair, K.W. (1971), “Further studies on flexural crack control in structural slab systems”, ACI SP-30, American Concrete Inst., Detroit, Mich., 1-41.

Owen, D.R.J. and Figueiras, J.A. (1984), “Ultimate load analysis of reinforced concrete plates and shells including geometric nonlinear effects”, In Finite element software for plates and shells, (Editors: E. Hinton and D.R.J. Owen), Pineridge Press, Swansea, U.K., 327-388.

Park, R. (1964), “Ultimate strength of rectangular concrete slabs under short term uniform loading with edges restrained against lateral movement”, *Proc., Institution of Civil Engrs.*, London, U.K., 125-150.

Wood, R.H. (1961), *Plastic and Elastic Design of Slabs and Plates*, Thames and Hudson, London.

Natation

The following symbols are used in this paper:

a	: aspect ratio of RC slab, L_y/L_x
b	: width to depth ratio of RC slab, L_x/h
h	: overall depth of RC slab
d	: effective depth of RC slab
f_{cu}	: concrete cube strength
f_c'	: concrete cylinder strength

f_y	: steel reinforcement yield strength
w	: experimental peak load
w_{p1}	: predicted peak load from FE-based Eq. (11)
w_{p2}	: predicted peak load from FE-based Eq. (14)
w_{p3}	: predicted peak load from MATLAB-based Eq. (17)
ρ	: Reinforcement ratio (in %)
α, β	: Non dimensional parameters
P, Q, u, v, y, z	: suitable constants determined for RC slab equation
A, B, C, D, E & F	: Equation constants identified by MATLAB